Article:

Kudzotsa, I, Dobbie, JS and Phillips, V (2019) Modeled aerosol-cloud indirect effects and processes based on an observed partially glaciated marine deep convective cloud case. Atmospheric Environment, 204. pp. 12-21. ISSN 1352-2310

https://doi.org/10.1016/j.atmosenv.2019.02.010

Modeled aerosol-cloud indirect effects and processes based on an observed partially glaciated marine deep convective cloud case

Innocent Kudzotsa[a], Steven Dobbie[b], Vaughan Phillips[c]

[a] *Finnish Meteorological Institute, Atmospheric Research Centre of Eastern Finland, P.O. Box 1627, 70211, Kuopio, Finland*
[b] *School of Earth and Environment, University of Leeds, LS2 9JT, Leeds, UK*
[c] *Department of Physical Geography and Ecosystem Science, Sölvegatan 12, S-223 62, Lund, Sweden*

Abstract

A tropical maritime case of deep convective clouds was studied using a state-of-the-art aerosol-cloud model in order to evaluate the microphysical mechanisms of aerosol indirect effects (AIE). The aerosol-cloud scheme used is a hybrid bin/bulk model, which treats all phases of clouds and precipitation allowing a detailed analysis of process-level aerosol indirect effects on targeted cloud types. From the simulations, a substantially huge total AIE on maritime clouds of -17.44 $\pm$6.1 Wm^{-2} was predicted primarily because maritime clouds are highly sensitive to perturbations in aerosol concentrations because of their low background aerosol concentrations. This was evidenced by the conspicuous increases in droplet and ice number concentrations and the subsequent reductions in particle mean sizes in the present-day. Both the water-only (-9.08 $\pm$3.18 Wm^{-2}) and the partially glaciated clouds (-8.36 $\pm$2.93 Wm^{-2}) contributed equally to the net AIE of these maritime clouds. As for the partially glaciated clouds, the mixed-phase component (-14.12 $\pm$4.94 Wm^{-2}) of partially glaciated clouds was dominant, whilst the ice-only component (5.76 $\pm$1.84 Wm^{-2}) actually exhibited a positive radiative forcing at the top of the atmosphere (TOA). This was primarily because ice water contents aloft were diminished significantly owing

☆Modeled aerosol-cloud indirect effects and processes based on an observed partially glaciated marine deep convective cloud case to increased snow production in the present-day.

Keywords: Aerosol-cloud interactions, partially glaciated clouds, atmospheric modelling, cloud microphysics, WRF model

---

Partially glaciated clouds are an integral part of the atmosphere, they are spatially and temporally ubiquitous and they have long lifetimes in the atmosphere mostly in the form of cirrus (Platt, 1973) and mixed-phase clouds (Verlinde et al., 2007; Shupe et al., 2008). On average, cirrus clouds are estimated to cover around 50 % of the tropical atmosphere (Prabhakara et al., 1993), while over 50 % of tropical rain is attributed to cloud systems that feature mixed-phase clouds (Liu, 2011). Cirrus clouds are usually remnants of deep convective clouds (DCC), while mixed-phase clouds are a common feature in cumulus congestus clouds (Sheffield et al., 2015) and DCCs (Storer and Van den Heever, 2013; Saleeby et al., 2016). Furthermore, DCCs are the atmosphere's conduit for transporting heat and moisture from the surface to the upper troposphere in the tropics (Fan et al., 2010). Tropical maritime cloud systems are of particular importance because of their immediate role in regulating the tropical atmospheric/oceanic circulation and sea surface temperatures SSTs (Evan et al., 2009; Li et al., 2010; Booth et al., 2012), all of which are key components of critical phenomena such as the ElNino Southern Oscilation (ENSO) (Holton and Dmowska, 1989), which is responsible for most of the global precipitation patterns (Ropelewski and Halpert, 1987; Dai and Wigley, 2000). It is therefore apparent that partially glaciated clouds/DCCs are an integral part of the Earth's hydrological and radiation budgets, nonetheless, it is not presently well understood how these of clouds are affected by changes in the loading of aerosols (Tao et al., 2012). The term partially glaciated clouds is used in this paper to mean clouds comprised of both mixed- and ice-only phases.

On the other hand, changes in atmospheric aerosol loadings, particularly anthropogenic-induced changes have profound effects on our climate since aerosols directly interact with solar radiation (Charlson et al., 1992; Haywood and Boucher, 2000; Rap et al., 2013) and also act as cloud condensation nuclei (CCN) or ice nuclei (IN) (Twomey, 1974; Albrecht, 1989; Lohmann and Feichter, 2005). As a result, an accurate representation of aerosols and associated processes is essential in improving climate forecasts (Carslaw et al., 2013), yet some important aerosol-cloud processes are presently not well understood and hence not well represented in numerical models, making aerosols the largest source of uncertainty in climate prediction (Boucher and Randall, 2013; Stevens, 2015; Carslaw and Johnson, 2018). It is therefore essential to improve our understanding of aerosol-cloud interactions, since the available literature indicates that the scattering and cloud nucleating aerosols impose a negative radiative forcing on climate and, hence, they have the potential to counteract the greenhouse effect (Solomon et al., 2007; Scott et al., 2014; Saleeby et al., 2016).

The objective of this study is therefore to investigate the key mechanisms by which changes in soluble aerosol loadings, which are a type CCN modify the microphysical properties of partially glaciated clouds in deep convective cloud systems of a tropical maritime environment. Tropical maritime convective clouds have been selected here because of their importance in atmospheric/oceanic circulation and global precipitation distribution and budget (Mann and Emanuel, 2006; Evan et al., 2009; Booth et al., 2012). Most of the studies that have been conducted so far have either focused on the effects of CCN on warm clouds or on the effects of CCN on isolated deep convective clouds (e.g., Martin et al., 1994; Cui et al., 2006) and (Tao et al., 2007; Hoeve et al., 2011; Lee et al., 2012; Costantino and Breon, 2013), while the effects of soluble aerosols on wider and long-lived convective cloud systems have received little attention (Gettelman et al., 2012). Therefore, we shall simulate multiple multi-cell mesoscale cloud systems in order to allow cell-to-cell interactions and feedbacks between clouds and their environment as opposed to simulations of isolated DCCs (Lohmann, 2002a; Khain et al., 2005; Connolly et al., 2006; Lee et al., 2009; Fan et al., 2012) or short-lived cloud systems (Saleeby et al., 2016) typically studied in the past.

Although this deficiency in our understanding of aerosol effects on partially glaciated clouds emanates partly from the large uncertainties associated with the measurements and knowledge of ice nucleating aerosols (Cziczo et al., 2004; DeMott et al., 2011) and our limited comprehension of mechanisms of ice nucleation (DeMott et al., 2010; Phillips et al., 2008, 2013) as opposed to cloud droplet nucleation (Kokkola et al., 2003; Petters and Kreidenweis, 2007; Romakkaniemi et al., 2014), the other daunting impediment to studying the aerosol interaction with partially glaciated clouds is the strong dependence of most ice-phase processes on warm-phase microphysics (Chen et al., 2017). For instance, an IN particle may be modified during the warm-phase before it nucleates ice and the presence of giant CCNs may inhibit ice processes by enhancing warm rain processes (Barahona et al., 2010). Therefore, in order to capture most of salient processes within this complex interface between the warm and the ice phases of convective clouds, we employ a state-of-the-art aerosol-cloud model (Kudzotsa et al., 2016a) that treats the microphysics of both the liquid (cloud droplets and rain) and solid (ice, snow and graupel) hydrometeor species. The aerosol-cloud scheme encapsulates a robust heterogeneous ice nucleation scheme of Phillips et al. (2008, 2013), which treats all the four known modes of heterogeneous ice nucleation (Diehl et al., 2001, 2002; Hoppel et al., 2002; Dymarska et al., 2006).

The structure of this article is as follows: Section. 1 provides a brief description of the model and then the model comparison with observations is presented in Section. 2. The microphysical responses of clouds to aerosol loading are presented and analysed in Section. 3, while the radiative responses of the clouds are presented in Section. 4 and conclusions are stated in the last section.

1. Model Description

Here we present a brief overview of the model description; the reader is referred to Kudzotsa (2013); Kudzotsa et al. (2016a) and references therein for the full description and validation of the aerosol-cloud model used in this study.

1.1. Overview and the Microphysics Scheme

The Cloud System Resolving Model (CSRM) used here was the Weather Research and Forecasting (WRF) model (Michalakes et al., 2005) Version 3.6

updated with a detailed aerosol-cloud scheme that is configured with hybrid bin/bulk microphysics (Kudzotsa, 2013; Kudzotsa et al., 2016a). The scheme comprises a two-moment treatment for the prognostic variables of all cloud and precipitation species and the dynamical framework was a non-hydrostatic and an-elastic fluid flow with periodic boundary conditions. The CSRM encapsulates an interactive radiation scheme from the geophysical fluid dynamics laboratory (GFDL) (Freidenreich and Ramaswamy, 1999).

Since the type of most of the clouds simulated in this study were of convective nature, the model top was set at 20 Km with a vertical level-spacing of 500 m. Although this spacing is seemingly coarse compared to other CSRMs, it is still about at least an order of magnitude smaller than the depth of the deep convective clouds that were simulated. In addition, the model uses a diagnosed value of supersaturation at the cloud base, hence it is sufficient to resolve the convective type of clouds simulated in this study. Also, the peak supersaturation close to cloud-base (typically about 10 meters above it) is parameterized with a dedicated cloud-base droplet activation scheme (Ming et al., 2006) and is not resolved, so there is little incentive for a finer vertical grid spacing to represent it. The domain was about 170 km wide in the east-west direction and simulated with a grid-spacing of 2 km. This spatial resolution is a trade-off between accuracy and computational expense whilst maintaining a relatively high temporal resolution of 10 seconds to be high enough to accurately resolve the time-dependent microphysical processes. A two-dimensional configuration was chosen for this study in order to minimize computational expense since according to Tompkins (2000) and Petch et al. (2008), two dimensional simulations are able to capture the key features of convective systems. Convection in the simulations is triggered by random perturbations of the moisture field at the beginning of the simulation and then maintained by tendencies of the observed large-scale forcing derived from the three-hourly soundings religiously launched during the campaign (May et al., 2008), while the temperature above the 15 km altitude was nudged back to observed profiles.

In this aerosol-cloud model, a total of seven different species were used as either cloud condensation (CCN), which are soluble or ice nuclei (IN), which are insoluble. The soluble aerosol species are ammonium sulphate (its bi-modal distribution is separated into two independent modes as $SO4_1$ and $SO4_2$), sea-salt (SS) and soluble organic carbonaceous material (SO), while the insoluble species were mineral dust/metallic (DM), soot/black carbon (BC), insoluble non-biological organic (O), primary biological aerosol particles (BIO) and finally, there is a fraction of the soluble organic group (SO) that becomes glassy at very cold temperatures (SOLO). They were all assumed to follow a bi-modal log-normal size distribution with the distribution parameters mostly constrained by observations (Kudzotsa et al., 2016a). The aerosol-cloud scheme tracks aerosols through all the processes that act as sinks (e.g. cloud activation and coagulation) and sources of aerosols such as droplet evaporation; however, it is beyond the capabilities of the model to simulate the natural replenishment of aerosols within the simulation domain. Therefore, an artificial technique for the replenishment of the aerosols within the simulation domain was applied by way of relaxing the aerosols profiles back to their initial values at intervals of three hours.

A Γ-distribution was used to describe both the precipitating and non-precipitating hydro-meteors. The nucleation of cloud droplets is treated explicitly using the Ming et al. (2006) scheme and the κ-Kohler theory of Petters and Kreidenweis (2007) depending on the type of nucleating particles and also on whether the nucleation is at cloud base or in-cloud. For the formation of ice crystals, an empirical parameterization (EP) of Phillips et al. (2008, 2013) was used. Other microphysical processes such as droplet growth by coagulation, ice multiplication, and auto-conversion are described in detail in Kudzotsa et al. (2016a). It is, however, important to highlight that a bin-emulating approach was applied for all the coagulation processes, while auto-conversion processes were treated using a bulk microphysics approach due to the difficulty associated with the explicit implementation of autoconversion, even in detailed microphysics models e.g, Tonttila et al. (2017). The bin-emulating approach is done by creating temporary grids with 33 bins in this case upon which the respective bulk concentrations of the interacting species are decomposed according to their assumed statical distributions. After the treatment of the targeted process is completed in this bin-emulating approach, the new bulk concentrations of the species are reassembled by summing up the discretized concentrations in each bin. This approach allows a bulk microphysics model to represent microphysics processes more realistically without much computational expense associated with full sectional microphysics models (Saleeby et al., 2016).

2. The Simulated Case

The model was used to simulate a maritime case of deep convection for two purposes: to evaluate its performance by comparing its predictions with observed quantities and to carry out sensitivity tests required to investigate the microphysical and dynamical mechanisms of aerosol indirect effects. The case that was simulated was the Tropical Warm Pool International Cloud Experiment (TWPICE), which was conducted over a period of one month, from the 17^{th} of January to the 12^{th} of February in 2006 over Darwin, in northwestern Australia (lat = -12.425° and lon = 130.891°). The surface of the domain was treated as completely maritime, with a constant sea surface temperature (SST) of 287 K being uniformly prescribed across the whole domain. This is consistent with what other researchers who have simulated the same experiment have applied (e.g; Fridlind et al., 2012). The The full details about this campaign are given in May et al. (2008); Fridlind et al. (2009); Kudzotsa (2013); Kudzotsa et al. (2016a).

In addition to the general specifications of the model given in Sect. 1.1, further specifications were applied in order to match the model conditions with the observed meteorological conditions and observing patterns used during the campaign. The model was initialized using the domain averages of observed thermodynamic (i.e. vapor and temperature) profiles from the TWPICE campaign. blue The time-mean state of the atmosphere was used to initialize the model for two reasons: firstly because averages filter out errors and anomalies in the observations and secondly, the simulations performed were two-dimensional.

The corresponding thermodynamic tendencies together with profiles of horizontal wind and pressure were used as large-scale forcing. The comparison of the model output with observed variables was rigorous since we compared the model cloud droplet, ice and aerosol number concentrations, in addition to other thermodynamic and microphysical fields such as temperature, humidity, water contents and precipitation.

Much of the description of the model performance and its validation are fully detailed in our previous work (e.g; Kudzotsa et al., 2016a), here we provide a brief description (without republishing the figures) that is necessary for the reader to contextualize the results in this paper. Several micro- and macrophysical parameters predicted by the model were compared with observations. These included the ice and cloud number concentrations together with profiles of the mean sizes. The mean cumulative precipitation and cloud fractions were also validated.

The comparison of the model predictions for the vertical profiles of ice and cloud number concentrations against observed values (Fig. 3 and Fig. 9 in Kudzotsa et al. (2016a), respectively) showed the model means lying within 90% confidence interval of the observations. It is fundamentally crucial in aerosol-cloud interactions research for the aerosol-cloud model to accurately treat the nucleation, growth and the interaction of these microphysical species with each other and the relatively close comparison exhibited by the model to observations makes it reliable. From the analysis of aerosol types that nucleated the ice, it was noted that dust particles were the dominant source of heterogeneously nucleated ice; however, soot and biological aerosol species showed substantial contributions to the total number concentration of heterogeneously nucleated ice. Homogeneous aerosol and cloud droplet freezing were by far the dominant sources of ice crystals, while the Hallett-Mossop process was the second most significant source of ice in the model. Similar satisfactory performance by the model was noted also in its prediction of other fields such as cloud cover, surface precipitation, and radiation fluxes.

The vertical profile of the mean domain-wide cloud fraction as shown in Fig.

14 of Kudzotsa et al. (2016a), shows that the model slightly under-predicted the mean cloud fraction in the lower troposphere by about 0.1 and mildly over-predicted in the middle-troposphere by about 0.1 to 0.2 in comparison to observations, while a near perfect agreement was exhibited in the upper troposphere. on average, the mean domain-wide cloud fraction of about 0.5 was predicted by the model in the middle troposphere. On the other hand, the time series of both the model and observations of cloud fraction during the whole simulation period show that the atmosphere was largely overcast during the first week of the simulation, while then after, although not overcast, there were significantly continuous cloud activities in the domain (Figure 1). As for the cumulative precipitation (Fig. 12 in Kudzotsa et al. (2016a)), a near-perfect agreement was exhibited, both in terms of amount and and trend of the precipitation curve. This is also important in showing that mass budget and boundary conditions are being treated properly in the model. The full evaluation of the model is given in Kudzotsa et al. (2016a).

3. The Responses of Clouds to Changes in Aerosol Loading

The sensitivity tests described fully in Kudzotsa et al. (2016b) were repeated in this work, hence, only a brief description of the tests is provided below. This paper only focuses on analyzing the responses of cloud properties to changes in aerosol loadings and on quantifying the corresponding radiative forcings of these clouds caused by changes in soluble aerosol loadings.

Test A of Kudzotsa et al. (2016b) comprised of two model runs, the only difference between the two simulations was in aerosol number concentrations. The simulation with present-day (i.e. 2010) aerosol concentration was designated as the control run and was denoted PD-CTRL, while the simulation in which the soluble aerosol burden was altered to pre-industrial levels (i.e. 1850) was designated as pre-industrial simulation and is denoted PI-SOL. In both simulations, the same present-day thermodynamic conditions were used to force the model as was done in other previous studies e.g. in Lohmann (2002a). The test was de-

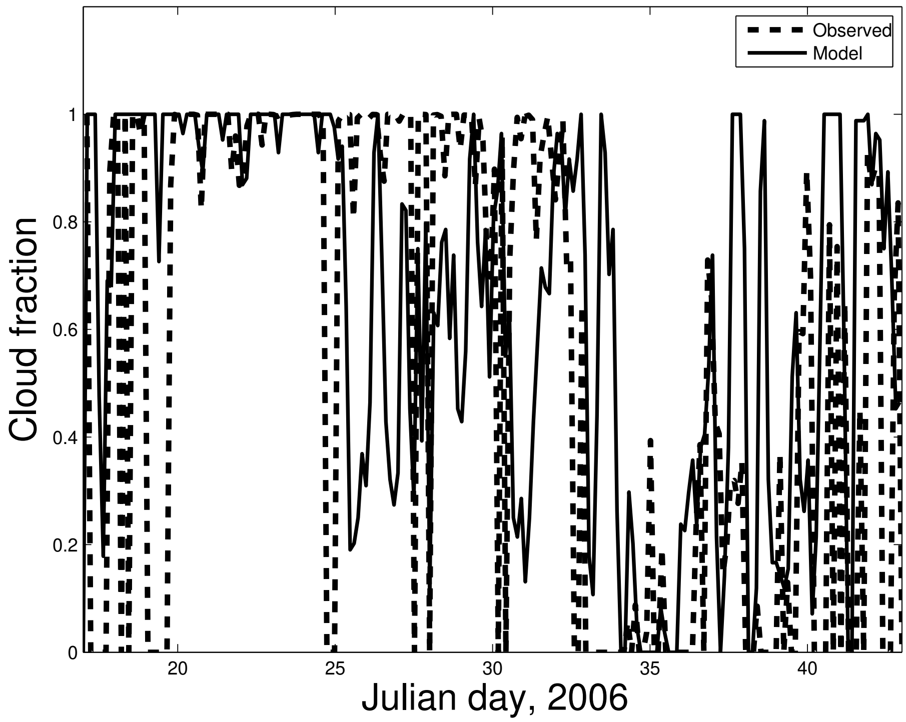

Figure 1: *Time series of cloud fraction for TWPICE averaged over the whole simulation domain for cloud mixing ratios greater than 0.01 gkg*$^{-3}$

signed to estimate the *effective total indirect effect*, F_{eff} due to soluble aerosols by differencing the top of the atmosphere (TOA) radiative fluxes of the PD-CTRL and the PI-SOL simulations (i.e. $TOA_{PD-CTRL}$ - TOA_{PI-SOL}). blue The present-day simulation was denoted the control simulation because the meteorological and micro-physical dataset used for model forcing and validation was derived from the present day.

Test B was designed to estimate the albedo-emissivity effect by calling the radiation scheme twice in both the PD-CTRL and the PI-SOL simulations. The difference between the first and the second calls is that in the first call, the radiation scheme is allowed to fully interact with clouds by using droplet information predicted in the simulation to calculate the radiative fluxes of clouds, while in the second call, the the radiation scheme uses information predefined lookup tables. The difference in the net radiative fluxes at the TOA between the control and the pre-industrial simulations determined using the these first calls to the radiation scheme gives the total or the effective net radiative flux, $F_{net} = F_{eff}$ as described on Test A. blue On the other hand, the second call to the radiation scheme is made for diagnostic purposes only (i.e., it does not alter the microphysics of the model). In the second call, the sensitivity of clouds to blue changes in aerosols is eliminated blue by using temperature-dependent look-up tables of the mean sizes of cloud droplets and ice crystals instead of the predicted mean sizes. These look-up tables are created from the control run (PD-CTRL described above), blue but they could equally be created also from the pr-industrial run. The same look-up tables are used for both PD-CTRL and PI-SOL runs. blue The difference in the net radiative fluxes at TOA between the control and the pre-industrial simulations determined using the these second calls to the radiation scheme gives a hypothetical net radiative flux minus the influence of changes in droplet properties, F_{hyp}. Finally, subtracting F_{hyp} from F_{eff}, gives us the estimate of the total albedo-emissivity effect from clouds, F_{alb}.

An important assumption made in these tests is that the effective total indirect effect, F_{eff}, is an arithmetic summation of the lifetime and albedo-emissivity effects, F_{alb} and the lifetime indirect effect. Therefore, from this assumption and the result derived from Test A and the albedo-emissivity effect from this Test B, the lifetime effect can be estimated as $F_{lif} = F_{eff}$ - F_{alb}. This Test B can be applied selectively on targeted cloud types and cloud processes in order to isolate their respective albedo and lifetime AIEs.

In order to examine how the simulated clouds responded to changes in soluble aerosol loadings, a number of microphysical and dynamical quantities representative of cloud characteristics are presented in this section. Some of these quantities are plotted as spatial and temporal bulk averages representing the whole system of simulated clouds, while other quantities are plotted as intrinsic averages. Intrinsic averages are evaluated by conditional averaging depending on the quantity being analysed; whether it is over cloudy regions, in which case, the condition would be cloud or ice mixing ratios greater than 0.001 gkg^{-1} or over deep convective or stratiform clouds, in which case a threshold of updraft speeds greater than 1 ms^{-1} or less than 1 ms^{-1} are applied respectively. This threshold for updraft speeds of deep convective clouds is equal to what was previously used by other researchers, for example by Sheffield et al. (2015), although it was much slower than what was predicted by Saleeby et al. (2016) and Fan et al. (2010), who applied updraft speeds of greater than 3 and 7 ms^{-1}, respectively. This is because they respectively simulated isolated DCCs and a single life-cycle mesoscale convective system.

Most of the plots presented here feature two curves, the dashed curve represents the simulation with present-day aerosol concentrations (PD-CTRL), which is the control simulation, while the solid curve represents the simulation with pre-industrial aerosol concentrations (PI-SOL). blue The vertical levels in the model are fixed in terms of height in meters. However, we included the mean temperature vertical axis in our figures in order to easily visualize and highlight some of the important temperature depended altitudes such as the melting and homogeneous freezing levels. The adjustment factors used to estimate the pre-industrial aerosol number concentrations were derived from the global model results of Takemura (2012) and are shown in Table. 1. blue Note that only soluble aerosol (CCN) species are shown in Table 1, whilst the solid or ice nucleating (IN) species are not shown. This is because IN number concentrations were not modified between the control and the pre-industrial simulations.

3.1. The Response of Cloud Microphysical Properties to Increased soluble Aerosols

3.1.1. Initiation of Cloud Droplets

Fig. 2a shows the simulated averages of the number concentrations of cloud droplets for both the present-day and the pre-industrial simulations and clearly, the concentrations of cloud droplets in the control simulation (PD-CTRL) is about four times higher than the pre-industrial simulation (PI-SOL). This relatively strong sensitivity to increases in aerosol loading is expected not only because there is a direct proportionality between activated cloud droplets and

Soluble Aerosol material	Adjustment Factor
Ammonium Sulphate (SO4)	0.19
Sea-Salt (SS)	1.
Soluble Organics (SO)	0.67

Table 1: *Fractional changes applied to present-day (2010) soluble aerosol number concentrations in order to represent the pre-industrial (1850) number concentrations (inferred from Takemura (2012)).*

the CCN concentrations in the CCN activity parameterization of Ming et al. (2006) used in the model, but also that other previous modelling and observational studies have shown this trend (Andreae et al., 2004; Boutle et al., 2018).

It was shown in our previous study that among the soluble aerosols, sulphate was by far the dominant source of cloud droplets followed by soluble organics. The accumulation mode of the bi-modal log-normal size distribution of sulphate aerosols dominated the droplet concentrations in the lower troposphere; however, in the upper troposphere, the smaller mode was an equally important source of cloud droplets (Kudzotsa et al., 2016a). It is important to note that the fractional increase in the cloud droplet loading and the fractional increase in the activated CCN concentration are not equivalent; the number concentration of the activated CCN is slightly higher than that of cloud droplets. This is expected because some of the cloud droplets grow by self-collection and some grow into precipitation (or rain drops) via collision-coalescence. In addition, the evaporation and homogeneous freezing of cloud droplets also account for this discrepancy. Finally, a corresponding monotonic reduction of about 5 μm in the mean sizes of cloud droplets was predicted in the present-day (Fig. 2b) owing to increased competition for available water vapor by more cloud droplets (Twomey, 1974).

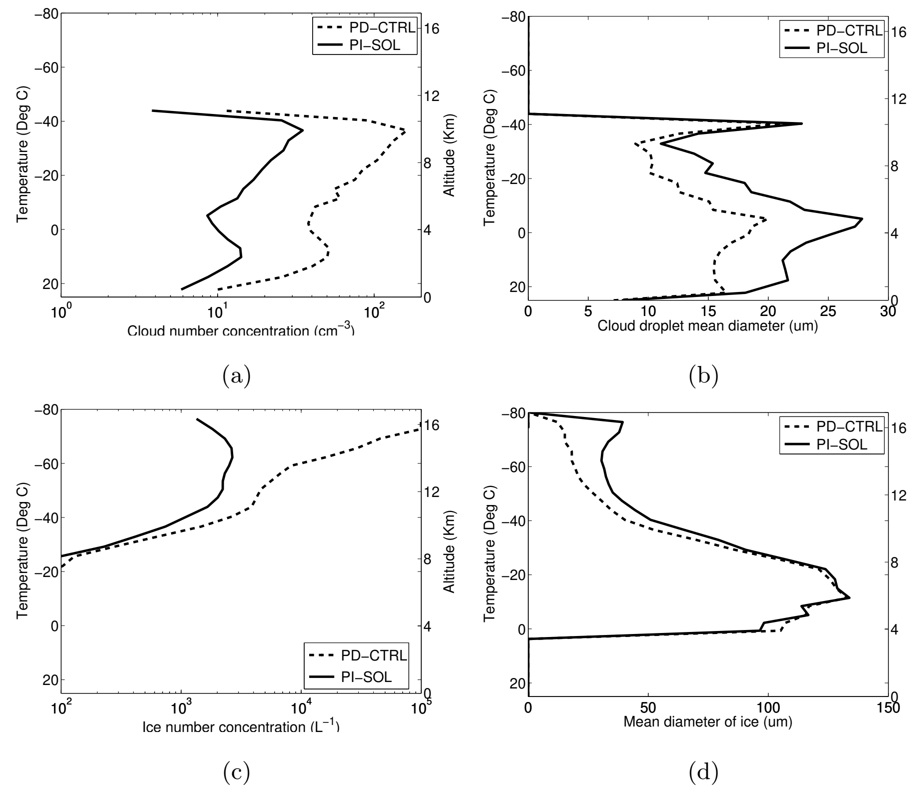

Figure 2: *(a) Cloud droplet number concentrations and (b) mean sizes of cloud droplets (c) ice crystal number concentrations and their corresponding effective sizes in (d). The quantities were conditionally averaged over cloudy conditions.*

3.1.2. Initiation of Cloud Ice

As for the total crystal concentrations (Fig. 2c), the fractional increase is insignificant in the lower troposphere but it diverges quite drastically from the preindustrial concentrations with increasing altitude owing mainly to the higher rates of homogeneous aerosol freezing exhibited in the present-day. A corresponding pattern in the reduction of effective sizes of ice crystals is shown in Fig. 2d. The average number concentration of ice crystals was about three orders of magnitude higher than the average number concentration of activated INP. This is a consequence of secondary mechanisms of ice formation such as homogeneous droplet/aerosol freezing and other ice multiplication processes such as the Hallett-Mossop (H-M) process. Similar findings from other tropical cases of deep convection were made by Phillips et al. (2007); Fan et al. (2010); Storelvmo et al. (2011). The ice number budget (Fig. 3) shows that homogeneous aerosol freezing, particularly of sulphate aerosols outnumbers all other sources of ice crystals, although it does not on its own, account for the total ice concentration. Crystals from homogeneous freezing of cloud droplets are much less than those from aerosol freezing. Other sources of ice crystals such as heterogeneous ice nucleation and the H-M splinters have smaller contribution to the overall ice concentrations.

0.5

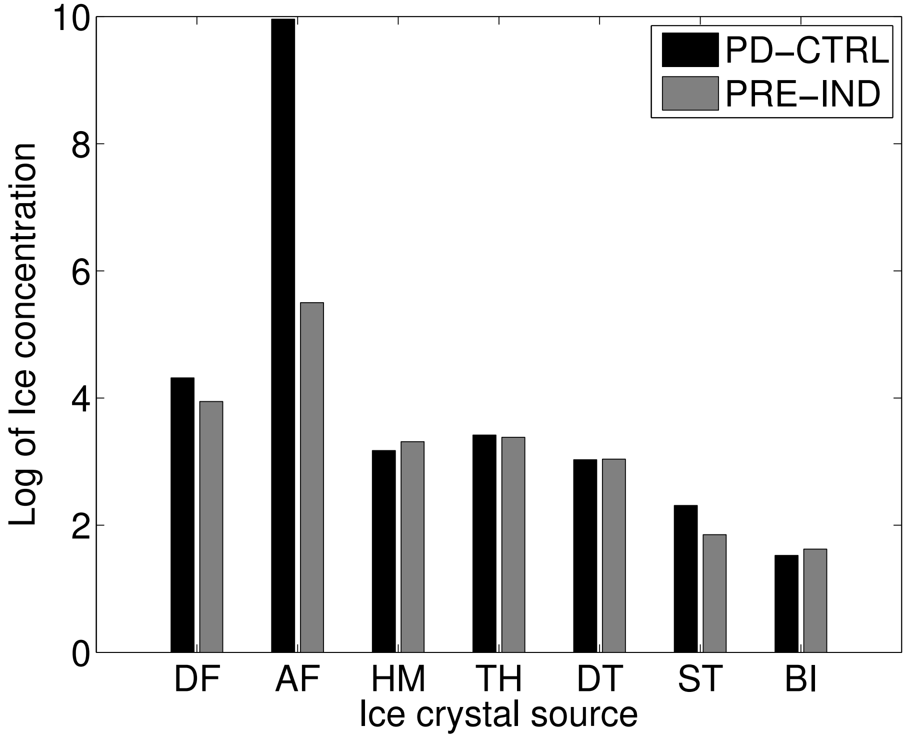

Figure 3: *The ice number budget from the simulation of TWPICE, DF = droplets frozen homogeneously, AF = aerosols frozen homogeneously, HM = H-M splinters, TH = total ice from heterogeneous nucleation, (DT, ST, BI) ice from heterogeneous nucleation of dust, soot and biological organics respectively.*

3.1.3. *Water Contents*

Figs. 4a and 4b show the liquid water content (LWC) and the ice water content (IWC) of clouds conditionally averaged over cloudy regions. A substantial monotonic increase of the LWC was evident in the control simulation owing to weakened present-day rain (Fig. 5) evident especially in surface precipitation (Fig. 5a) and mixed-phase clouds (Fig. 5b). This weakening in rain production is a direct consequence of predicted strong reduction in present-day droplet mean sizes. The weak precipitation production implies that more liquid water stays longer in the cloud thereby extending the lifetime of the clouds.

As for the ice water content, there was barely any change between the freezing and the homogeneous freezing levels, although a strong reduction of the upper-tropospheric IWC was consequently predicted in the present-day simulation, especially in regions of weak vertical velocities. The primary mechanisms for this reduction in the upper-tropospheric IWC were the increase of snow production in regions of deep convective clouds and the reduced detrainment of ice from the convective cores into cirrus which was indicated by the general weakening of cloud updrafts in the present day. In regions where vertical velocity remain the same, it ordinarily implies that there was no additional buoyancy created from the latent heating, i.e. the lack of the invigoration effect (Khain et al., 2005).

3.1.4. *Precipitation*

There was overall, no substantial change in the rain mixing ratio arising from the inclusion of aerosol pollution (Figs. 5a), although there is a significant bias towards weakening of rain production especially when rain reaching the ground is considered. The dominant contribution to this reduction in the overall rain was from present-day mixed-phase clouds (Fig. 5b). This indicates that there was small perturbation to the collision-coalescence process in these clean maritime clouds that resulted from increased soluble aerosols, even though there was a significant reduction in the mean sizes of cloud droplets.

On the other hand, the intrinsic (or the conditionally averaged) snow produc-

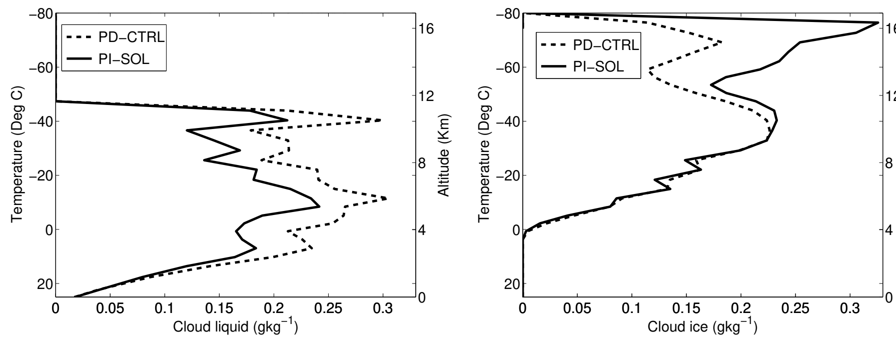

(a) (b)

Figure 4: *(a) Liquid water content, (b) ice water content conditionally averaged over cloudy regions and in regions of weak ascent.*

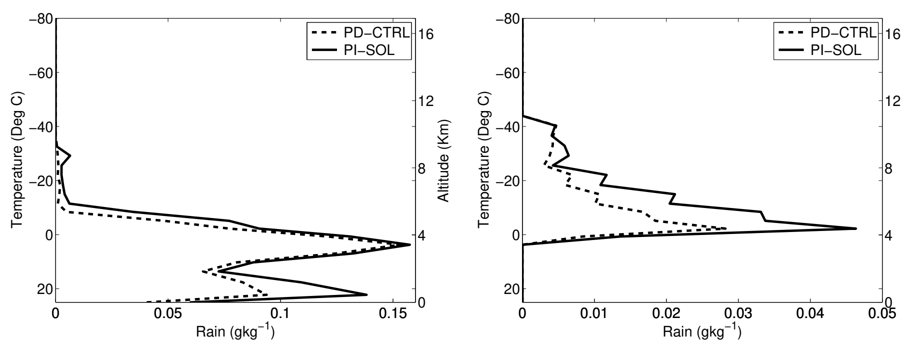

(a) (b)

Figure 5: *Rain mass mixing ratios conditionally averaged over (a) liquid-only clouds and (b) mixed-phase clouds in TWPICE. Liquid-only clouds are mathematically defined when in a given grid-box, only the water mixing ratio is greater than 0.001 gkg^{-1}, while for mixed-phase clouds, both the water and the ice mixing ratios must be greater 0.001 gkg^{-1}.*

tion in the present-day was heavily suppressed by the increases in soluble aerosol, especially in stratiform ice-only clouds, which are also the dominant contributor to the ice-only cloud fraction and hence, these clouds had more influence on the microphysical properties of all ice-only clouds than deep-convective clouds. This suppression of snow is attributed to the strong reduction in mean sizes of ice-crystal in the upper-troposphere. In addition, there was also a significant reduction of supersaturations in the regions of weak vertical velocities, which also limits the growth of snow. As for the production rates of graupel, there was hardly any change noted in all cloud types in these simulations. This weakening of precipitation with increasing aerosol loading is in keeping with other studies e.g. (Storer et al., 2010) who investigated the effects of aerosols on convective clouds under different thermodynamic environments.

3.1.5. Vertical Velocities, Cloud Cover and Optical Thickness

There is a complex interplay between the dynamics and the microphysics of a cloud; at a macrophysical level, the dynamics determine the depth and spatial extent of the cloud, while on the microphysical scale, the dynamics control the degree of supersaturation in a cloud and to a certain extent the collection efficiencies of cloud particles during growth by collision-coalescence and aggregation processes (if the geometric sweep-out concept is taken into consideration) (Phillips et al., 2014). blue There was a significant weakening of vertical velocities in the present-day especially in the upper troposphere for regions of weak ascent (Fig. 6a) and in the middle troposphere for regions of strong ascent (Fig 6b). This was in tandem with the reduction in upper-tropospheric IWC and LWC in general (Fig. 4). The reduction in IWC can imply suppression of latent heat released during freezing, which essentially weakens the strength of updrafts. In addition, the predicted increase in LWC is an indication of little to no partitioning of liquid-phase clouds to ice clouds and this has the same effect reducing the strength of updrafts.

3.1.6. Cloud Fractions

As for the horizontal cloud fractions (Fig. 7a), a net increase in total cloud fraction of about 5% was predicted and also a general increase across all cloud types was predicted in the present-day. This alludes to the fact that overall, all the cloud regimes became horizontally more extensive. blue Note that the sum of individual cloud covers of specific cloud phases exceeds the cloud fraction for all clouds. This is because of the overlaps in spatial coverage by these cloud types

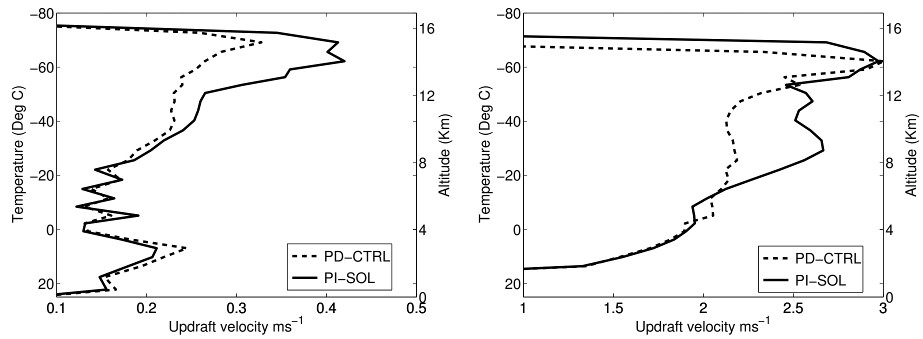

(a) (b)

Figure 6: *Vertical velocity profiles conditionally averaged over clouds with, (a) weak vertical velocities and (b) strong vertical velocities. For weak vertical velocities, the vertical velocity is less 1 m s^{-1} while it is greater than 1 m s^{-1} for strong vertical velocities.*

caused mainly by their occurrence at different altitudes. Further investigation also indicated that all the cloud types became more extensive in the present-day because the volumetric cloud fraction (the fraction of the grid boxes in the whole domain that have clouds) showed an escalation of the number of cloudy grid-boxes for virtually all the cloud types, especially for mixed-phase clouds and followed by ice-only clouds (Fig. 7b). As a result, both the intrinsic and the domain averaged optical thicknesses of all cloud types (Fig. 8) exhibited a large percentage increase due to aerosol perturbation. This conspicuous change in the optical properties of clouds implies that the cloud reflectance was also strongly altered. All the noted microphysical changes such as an increase in droplet and ice number concentrations and the reductions in mean particle sizes, in addition to precipitation suppression are perfect ingredients for increased cloud fractions and optical thicknesses (Twomey, 1974, 1977).

4. Response of Radiative Fluxes and Cloud Radiative Properties to Increased soluble Aerosols

This section presents analysis and discussion of how the modifications of micro- and macrophysical properties of clouds by the increase in soluble aerosols

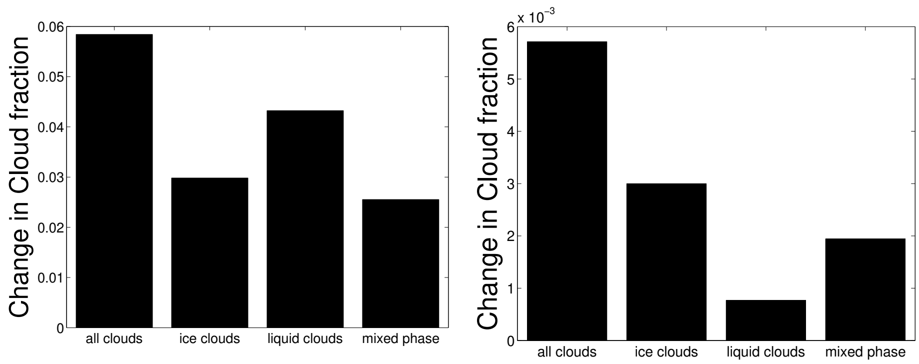

(a) (b)

Figure 7: *(a). The change in cloud fraction for all types of cloud species in TWPICE. (b). The change in volumetric cloud fraction for all types of cloud species in TWPICE.*

affect the radiative properties of clouds and their corresponding net radiative forcing for this domain. This was done by analyzing the changes of the radiative fluxes at the top of the atmosphere.

Figure 9 presents the radiative flux changes at the TOA caused by anthropogenic increases in the loadings of aerosols between the pre-industrial and the present-day eras. The modelling results show a strong negative radiative forcing from all the clouds at the TOA (-17.44 $\pm$6.1 Wm^{-2}). This is because maritime atmospheres are characterized by low background concentrations of aerosols, which makes them very sensitive to any changes in the aerosol field. Background aerosol loading refers to the average pre-industrial aerosol concentration. The sensitivity to aerosol changes in any atmosphere or any cloud regime decreases as the background aerosol concentration increases because a saturation point can be reached beyond which the sensitivity to aerosol perturbations becomes minimal. This result corroborates the finding of Andreae et al. (2007) who discovered that the aerosol indirect effects are larger in clean clouds than in polluted clouds. In other words, maritime clouds are expected to be more sensitive to aerosol changes than continental clouds. In our recent previous study (Kudzotsa et al., 2016b) where we investigated the effects of soluble aerosols on continental clouds, we predicted a smaller net indirect effect

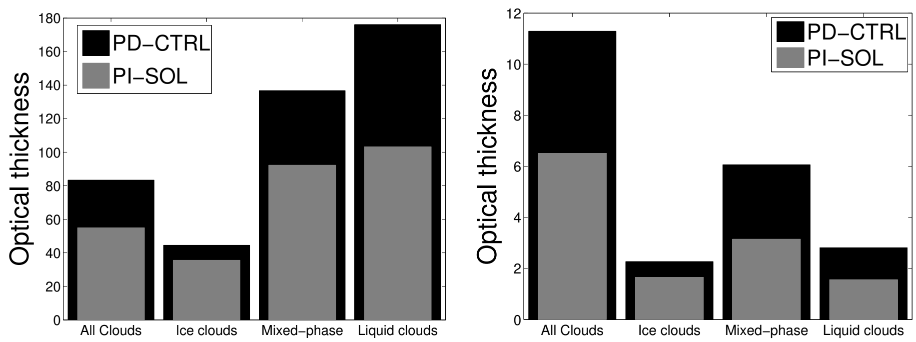

(a) (b)

Figure 8: *Superimposed optical thicknesses predicted in the TWPICE simulation; (a) conditionally averaged over grid-boxes in which the mass mixing ratio of a targeted cloud type is greater than blue 0.001 gkg*$^{-1}$ *and (b) unconditionally averaged over the entire domain and duration of the simulation. Optical depth from each cloud-type is plotted by assuming that no other cloud-types are present.*

of about $-9.Wm^{-2}$ over a similar domain and from similar cloud types.

The primary contributions to this strong aerosol indirect effect were the distinct increases in droplet number concentrations by about a factor of five and the doubling of ice crystal number concentrations in the upper-troposphere. Also, the substantial perturbation of other microphysical properties such as the optical thickness and increase in cloud cover caused this huge AIE. Fig. 8 clearly shows that the present-day clouds are very optically thick compared to the pre-industrial clouds.

Both the water-only (AIE of -9.08 $\pm$3.18 Wm^{-2}) and the partially glaciated clouds (AIE of -8.36 $\pm$2.93 Wm^{-2}) have shown equal importance in contributing to the net AIE of all clouds. This is primarily due to the fact that there was a strong increase in the number concentrations of both cloud and ice particles and a corresponding reduction in their respective mean sizes of these clouds. In addition, water clouds possess a strong radiative signature, especially in the shortwave region of the electromagnetic radiation spectrum, while ice clouds exist vertically above water clouds, and hence having the first interaction with solar radiation; thus, any change to their properties contributes significantly to

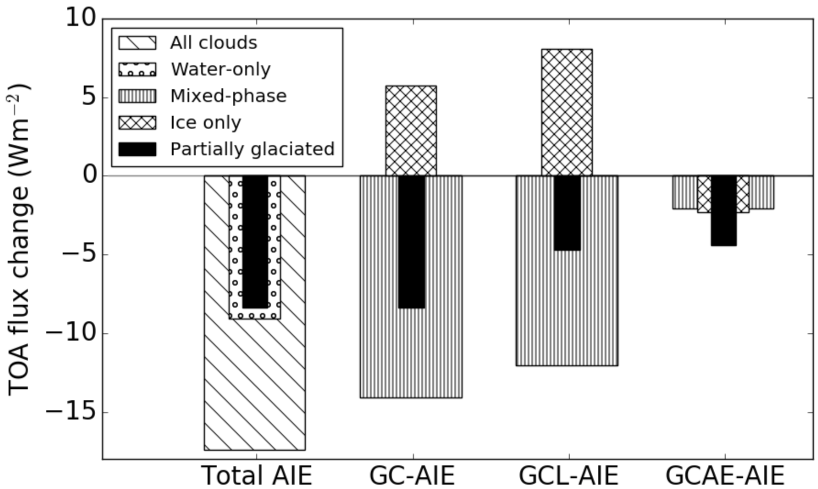

Figure 9: *The aerosol indirect effects (AIE) from soluble aerosols calculated for different cloud phases. Meaning of abbreviations: Total AIE = Total aerosol indirect effect from all clouds. GC-AIE = AIE from partially glaciated clouds, GCL-AIE = The lifetime indirect effect from partially glaciated clouds, GCAE-AIE = The albedo-emissivity indirect effect from partially glaciated clouds.*

the overall AIEs.

For the partially glaciated clouds aerosol indirect effect, the mixed-phase component (-14.12 $\pm$4.94 Wm^{-2}) of partially glaciated clouds was dominant, whilst in fact the ice-only clouds component (5.76 $\pm$1.84 Wm^{-2}) exhibited a positive radiative flux change at the TOA. The predicted reduction in uppertropospheric IWC implies that ice-only clouds allowed more solar radiation into the atmosphere.

The albedo-emissivity effects and the lifetime indirect effects for the partially glaciated clouds had a comparable cooling effect of -4.4 $\pm$1.54 Wm^{-2} and -4.5 $\pm$1.54 Wm^{-2}, respectively. The reduction in the droplet sizes and the increase in the number concentrations of the cloud droplets made them more reflective causing such a cooling.

In this work, we investigated the microphysical and dynamical effects of aerosols on clouds, caused by anthropogenic increases in aerosol concentrations that occurred between the preindustrial and the present-day eras and the ensuing effects that these changes have on the radiative properties of clouds with our main focus having been on tropical maritime partially glaciated clouds. The investigation was conducted using a state-of-the-art aerosol-cloud model that included aerosols of different chemical compounds that are either internally or externally mixed. We conducted various sensitivity tests to isolate different aerosol indirect effects.

Our results predicted a factor of four increase in the cloud droplet number concentrations caused by aerosol pollution because in pristine environments such as in the simulated case, droplet concentrations are more sensitive to aerosol concentrations than in a polluted case where cloud droplet concentrations are driven more by updraft speeds and the thermodynamic conditions. The water contents of clouds in the simulated case were relatively low compared to what is generally expected in a continental scenario e.g Kudzotsa et al. (2016a). This was mainly because precipitation efficiency is generally high in maritime clouds because of low concentrations of aerosol particles that characterize maritime atmospheres. As a result, fewer cloud particles are activated which can easily grow into large sizes and consequently, precipitation. Overall, the LWC slightly increased with increased aerosol concentrations, while the IWC in the upper-troposphere diminished quite significantly in the present-day simulation. Although the particle sizes diminished with aerosol pollution, the reduction was moderate and consequently, the microphysical processes (such as collision-coalescence, riming and aggregation) that are particle size dependent were not strongly altered.

The total aerosol indirect effect from all clouds of about -17.44 $\pm$6.1 Wm^{-2} was predicted in this marine case when soluble aerosols were increased from pre-industrial to present day. This is a huge radiative forcing that was caused mainly by the high sensitivity of maritime clouds to perturbations in aerosol concentrations. This derives from the fact that the aerosol indirect effect increases as the background aerosol concentration decreases. This explanation is in agreement with the findings of Kudzotsa et al. (2016a) in which a continental case was simulated and the total aerosol indirect effect of about -9 Wm^{-2} was predicted over an equal domain size and similar convective clouds and similarly in Andreae et al. (2007). Both the partially glaciated and the water-only clouds in this case contributed equally to the total aerosol indirect effect of clouds. For the water-only clouds, this was attributed to their high sensitivity to aerosol loading and also to their strong radiative signature especially on shortwave radiation. Whereas partially glaciated clouds had a significant contribution because of their existence vertically above the water clouds and therefore they interact with radiation first before it reaches water clouds.

The main conclusions drawn from this study pertaining to the radiative properties of clouds are: (1) The total aerosol indirect effect from all clouds was large (-17.44 $\pm$6.1 Wm^{-2}) and this is characteristic of environments with pristine background aerosols. (2) Both the water-only and the partially glaciated clouds contributed equally to the net AIEs. (3) The component of ice-only clouds in the total AIE was a positive radiative flux change at the TOA while that of the mixed-phase clouds was a negative radiative flux change, which subsequently dominated the AIE of partially glaciated clouds. (4) Finally, the magnitude of the albedo-emissivity effect was comparable to the lifetime AIE.

Acknowledgements

The work was funded by an award to Vaughan T. J. Phillips (VTJP) from Office of Science (BER), US Department of Energy (DE-SC0002383, which later became DE-SC0007396).

References

Albrecht B. Aerosols, cloud microphysics, and fractional cloudiness, science. Science 1989;245(4923):1227–30.

Andreae MO, Rosenfeld D, Artaxo P, Costa AA, Frank GP, Longo KM, Silva-Dias MAF. Smoking rain clouds over the amazon. Science 2004;303(5662):1337–42.

Andreae MO, et al. Aerosols before pollution. Science(Washington) 2007;315(5808):50–1.

Barahona D, West R, Stier P, Romakkaniemi S, Kokkola H, Nenes A. Comprehensively accounting for the effect of giant ccn in cloud activation parameterizations. Atmospheric Chemistry and Physics 2010;10(5):2467–73.

Booth BB, Dunstone NJ, Halloran PR, Andrews T, Bellouin N. Aerosols implicated as a prime driver of twentieth-century north atlantic climate variability. Nature 2012;484(7393):228.

Boucher O, Randall D. Climate change 2013: The physical science basis. contribution of working group i to the fifth assessment report of the intergovernmental panel on climate change, (ipcc). Cambridge University Press, Cambridge, United Kingdom and New York, NY, USA 2013;5th.

Boutle I, Price J, Kudzotsa I, Kokkola H, Romakkaniemi S. Aerosol–fog interaction and the transition to well-mixed radiation fog. Atmospheric Chemistry and Physics 2018;18(11):7827–40. URL: https://www.atmos-chem-phys.net/18/7827/2018/. doi:10.5194/acp-18-7827-2018.

Carslaw K, Lee L, Reddington C, Pringle K, Rap A, Forster P, Mann G, Spracklen D, Woodhouse M, Regayre L, et al. Large contribution of natural aerosols to uncertainty in indirect forcing. Nature 2013;503(7474):67.

Carslaw K. S. LALLAR, Johnson JS. Climate models are uncertain, but we can do something about it. Eos 2018;99.

Charlson R, Schwartz SE, Hales J, Cess R, Coakley JJ, JE. H, DJ. H. Climate forcing by anthropogenic aerosols. Science 1992;255(5043):423–30.

Chen Q, Koren I, Altaratz O, Heiblum RH, Dagan G, Pinto L. How do changes in warm-phase microphysics affect deep convective clouds? Atmospheric Chemistry and Physics 2017;17(15):9585–98.

Connolly PJ, Choularton TW, Gallagher MW, Bower KN, Flynn MJ, Whiteway JA. Cloud-resolving simulations of intense tropical hector thunderstorms: Implications for aerosol-cloud interactions. QJR Meteorol Soc 2006;132:3079–106. doi:10.1256/qj.05.86.

Costantino L, Breon FM. Aerosol indirect effect on warm clouds over south-east atlantic, from co-located modis and calipso observations. Atmospheric Chemistry and Physics 2013;13:69–88.

Cui Z, Carslaw KS, Yin Y, Davies S. A numerical study of aerosol effects on the dynamics and microphysics of a deep convective cloud in a continental environment. J Geophys Res 2006;111(D05):D05201.

Cziczo DJ, Murphy DM, Hudson PK, Thomson DS. Single particle measurements of the chemical composition of cirrus ice residue during crystal-face. J Geophys Res 2004;109:D04201.

Dai A, Wigley T. Global patterns of enso-induced precipitation. Geophysical Research Letters 2000;27(9):1283–6.

DeMott PJ, M6hler O, Stetzer O, Vali G, Levin Z, Petters MD, Murakami M, Leisner T, Bundke U, Klein H, Kanji ZA, Cotton R, Jones H, Benz S, Brinkmann M, Rzesanke D, Saathoff H, Nicolet M, Saito A, Nillius B, Bingemer H, Abbatt J, Ardon Karin. an dGanor E, Georgakopoulos DG, Saunders C. Resurgence in ice nuclei measurement research. Bull Amer Meteor Soc 2011;92:1623–35.

DeMott PJ, Prenni AJ, Liu X, Kreidenweis SM, Petters MD, Twohy CH, Richardson M, Eidhammer T, Rogers D. Predicting global atmospheric ice nuclei distributions and their impacts on climate. Proceedings of the National Academy of Sciences 2010;107(25):11217–22.

Diehl K, Matthias-Maser S, Jaenicke R, Mitra S. The ice nucleating ability of pollen:: Part ii. laboratory studies in immersion and contact freezing modes. Atmospheric research 2002;61(2):125–33.

Diehl K, Quick C, Matthias-Maser S, Mitra S, Jaenicke R. The ice nucleating ability of pollen: Part i: Laboratory studies in deposition and condensation freezing modes. Atmospheric Research 2001;58(2):75–87.

Dymarska M, Murray BJ, Sun L, Eastwood ML, Knopf DA, Bertram AK. Deposition ice nucleation on soot at temperatures relevant for the lower troposphere. Journal of Geophysical Research: Atmospheres (1984–2012) 2006;111(D4).

Evan AT, Vimont DJ, Heidinger AK, Kossin JP, Bennartz R. The role of aerosols in the evolution of tropical north atlantic ocean temperature anomalies. Science 2009;324(5928):778–81.

Fan J, Comstock JM, Ovchinnikov M. The cloud condensation nuclei and ice nuclei effects on tropical anvil characteristics and water vapor of the tropical tropopause layer. Environmental Research Letters 2010;5(4):044005.

Fan J, Rosenfeld. D, Yanni Ding L, Leung. R, Li Z. Potential aerosol indirect effects on atmospheric circulation and radiative forcing through deep convection. Geophysical Research Letters 2012;39(9):L09806.

Freidenreich SM, Ramaswamy V. A new multiple-band solar radiative parameterization for general circulation models. J Geophys Res 1999;104(D24):31389–409.

Fridlind A, Ackerman A, Chaboureau JP, Fan J, Grabowski WW, Hill A, Jones T, Khaiyer M, Liu G, Minnis P, et al. A comparison of twp-ice observational data with cloud-resolving model results. Journal of Geophysical Research: Atmospheres 2012;117(D5).

Fridlind A, Andrew A, Jon P, Paul F, Hill A, Greg M, Shaocheng X, Minghua Z. Arm/gcss/sparc twp-ice crm intercomparison study; 2009. TWP-ICE technical report.

Gettelman A, Liu X, Barahona D, Lohmann D, Chen C. Climate impacts of ice nucleation. Journal of Geophysical Research: Atmospheres 2012;117(D20):D20201.

Haywood J, Boucher O. Estimates of the direct and indirect radiative forcing due to tropospheric aerosols: A review. Reviews of Geophysics 2000;38(4):513–43.

Hoeve TJE, Remer LA, Jacobson MZ. Microphysical and radiative effects of aerosols on warm clouds during the amazon biomass burning season as observed by modis: impacts of water vapor and land cover. Atmos Chem Phys 2011;11:3021–36.

Holton JR, Dmowska R. El Niño, La Niña, and the southern oscillation. volume 46. Academic press, 1989.

Hoppel WA, Frick GM, Fitzgerald JW. Surface source function for sea-salt aerosol and aerosol dry deposition to the ocean surface. Journal of Geophysical Research: Atmospheres 2002;107(D19):AAC 7–1. URL: `http://dx.doi.org/10.1029/2001JD002014`. doi:`10.1029/2001JD002014`.

Khain A, Rosenfeld D, Pokrovsky A. Aerosol impact on the dynamics and microphysics of deep convective clouds. Quarterly Journal of the Royal Meteorological Society 2005;131:2639–63.

Kokkola H, Romakkaniemi S, Kulmala M, Laaksonen A. A cloud microphysics model including trace gas condensation and sulfate chemistry. Boreal environment research 2003;8(4):413–24.

Kudzotsa I. Mechanisms of Aerosol Indirect Effects on Glaciated Clouds Simulated Numerically. Ph.D. thesis; University of Leeds, UK; 2013.

Kudzotsa I, Phillips VJP, Dobbie S, Formenton M, Sun J, Allen G, Bansemer A, Spracklen D, Pringle K. Aerosol indirect effects on glaciated clouds. part i: Model description. QJRMS 2016a;.

Kudzotsa I, Phillips VJP, Dobbie S, Marco. . Aerosol indirect effects on glaciated clouds. part ii: Sensitivity tests. QJRMS 2016b;.

Lee SS, Donner LJ, Phillips V. Sensitivity of aerosol and cloud effects on radiation to cloud types: comparison between deep convective clouds and warm stratiform clouds over one-day period. Atmos Chem Phys 2009;9:2555–75.

Lee SS, Graham F, Chuang PY. Effect of aerosol on cloud-environment interactions in trade cumulus. J Atmos Sci 2012;69:3607–32.

Li H, Dai A, Zhou T, Lu J. Responses of east asian summer monsoon to historical sst and atmospheric forcing during 1950–2000. Climate Dynamics 2010;34(4):501–14.

Liu C. Rainfall contributions from precipitation systems with different sizes, convective intensities, and durations over the tropics and subtropics. Journal of Hydrometeorology 2011;12(3):394–412.

Lohmann U. A glaciation indirect aerosol effect caused by soot aerosols. Geophysical Research Letters 2002a;29. doi:`10.1029/2001GL014357`.

Lohmann U, Feichter J. Global indirect aerosol effects: a review. Atmospheric Chemistry and Physics 2005;5(3):715–37. URL: `http://www.atmos-chem-phys.net/5/715/2005/`. doi:`10.5194/acp-5-715-2005`.

Mann ME, Emanuel KA. Atlantic hurricane trends linked to climate change. Eos, Transactions American Geophysical Union 2006;87(24):233–41.

Martin G, Johnson D, Spice A. The measurement and parameterization of effective radius of droplets in warm stratocumulus clouds. Journal of the Atmospheric Sciences 1994;51(13):1823–42.

May PT, Mather JH, Geraint V, Keith N. B, Christian J, Greg M. M, Gerald G. M. The tropical warm pool international cloud experiment. American Meteorological Society 2008;89:629–45. doi:`http://dx.doi.org/10.1175/BAMS-89-5-629`.

Michalakes J, Dudhia J, Gill D, Henderson T, Klemp J, Skamarock W, Wang W. The weather research and forecast model: software architecture and performance. In: Use of High Performance Computing in Meteorology. World Scientific; 2005. p. 156–68.

Ming Y, Ramaswamy V, Donner LJ, Phillips VTJ. A new parameterization of cloud droplet activation applicable to general circulation models. Journal of the atmospheric sciences 2006;63:1348–56.

Petch J, Blossey P, Bretherton C. Differences in the lower troposphere in two- and three-dimensional cloud-resolving model simulations of deep convection. Quarterly Journal of the Royal Meteorological Society 2008;134(636):1941–6.

Petters MD, Kreidenweis SM. A single parameter representation of hygroscopic growth and cloud condensation nucleus activity. Atmospheric Chemistry and Physics 2007;7(8):1961–71. URL: http://www.atmos-chem-phys.net/7/1961/2007/. doi:10.5194/acp-7-1961-2007.

Phillips VTJ, DeMott PJ, Andronache C. An empirical parameterization of heterogeneous ice nucleation for multiple chemical species of aerosol. Journal of the atmospheric sciences 2008;65:2757–83. doi:10.1175/2007JAS2546.1.

Phillips VTJ, Demott PJ, Andronache C, Pratti KA, Twohy C. Improvements to an empirical parameterization of heterogeneous ice nucleation and its comparison with observations. J Atmos Sci 2013;70:378–409.

Phillips VTJ, Donner LJ, Garner ST. Nucleation processes in deep convection simulated by a cloud-system-resolving model with double-moment bulk microphysics. Journal of the Atmospheric Sciences 2007;64:738–61. doi:http://dx.doi.org/10.1175/JAS3869.1.

Phillips VTJ, Formenton M, Lienert B, Kudzotsa I. A parameterisation of sticking efficiency for collisions of graupel and snow with ice crystals: Theory and comparison with observations. JGR 2014;.

Platt C. Lidar and radiometric observations of cirrus clouds. Journal of the atmospheric sciences 1973;30(6):1191–204.

Prabhakara C, Kratz D, Yoo JM, Dalu G, Vernekar A. Optically thin cirrus clouds: Radiative impact on the warm pool. Journal of Quantitative Spectroscopy and Radiative Transfer 1993;49(5):467–83.

Rap A, Scott CE, Spracklen DV, Bellouin N, Forster PM, Carslaw KS, Schmidt A, Mann G. Natural aerosol direct and indirect radiative effects. Geophysical Research Letters 2013;40(12):3297–301.

Romakkaniemi S, Jaatinen A, Laaksonen A, Nenes A, Raatikainen T. Ammonium nitrate evaporation and nitric acid condensation in dmt ccn counters. Atmospheric Measurement Techniques 2014;7(5):1377–84.

Ropelewski CF, Halpert MS. Global and regional scale precipitation patterns associated with the el niño/southern oscillation. Monthly weather review 1987;115(8):1606–26.

Saleeby S, Heever S, Marinescu P, Kreidenweis S, DeMott P. Aerosol effects on the anvil characteristics of mesoscale convective systems. Journal of Geophysical Research: Atmospheres 2016;121(18).

Scott C, Rap A, Spracklen D, Forster P, Carslaw K, Mann G, Pringle K, Kivekäs N, Kulmala M, Lihavainen H, et al. The direct and indirect radiative effects of biogenic secondary organic aerosol. Atmospheric Chemistry and Physics 2014;14(1):447–70.

Sheffield AM, Saleeby SM, Heever SC. Aerosol-induced mechanisms for cumulus congestus growth. JGR: Atmospheres 2015;120(17):8941–52.

Shupe MD, Daniel JS, De Boer G, Eloranta EW, Kollias P, Long CN, Luke EP, Turner DD, Verlinde J. A focus on mixed-phase clouds: The status of ground-based observational methods. Bulletin of the American Meteorological Society 2008;89(10):1549–62.

Solomon S, Qin D, Manning M, Chen Z, Marquis M, Averyt K, M.Tignor , (eds.) HM. Climate change 2007: The physical science basis. contribution of working group i to the fourth assessment report of the intergovernmental panel on climate change, (ipcc). Cambridge University Press, Cambridge, United Kingdom and New York, NY, USA 2007;4th.

Stevens B. Rethinking the lower bound on aerosol radiative forcing. Journal of Climate 2015;28(12):4794–819.

Storelvmo T, Hoose C, Eriksson P. Global modeling of mixed-phase clouds: The albedo and lifetime effects of aerosols. Journal of Geophysical Research: Atmospheres 2011;116(D5).

Storer RL, Van den Heever SC. Microphysical processes evident in aerosol forcing of tropical deep convective clouds. Journal of the Atmospheric Sciences 2013;70(2):430–46.

Storer RL, Van Den Heever SC, Stephens GL. Modeling aerosol impacts on convective storms in different environments. Journal of the Atmospheric Sciences 2010;67(12):3904–15.

Takemura T. Distributions and climate effects of atmospheric aerosols from the preindustrial era to 2100 along representative concentration pathways (rcps) simulated using the global aerosol model sprintars. Atmos Chem Phys 2012;12:11555–72.

Tao WK, Chen JP, Li Z, Wang C, Zhang C. Impact of aerosols on convective clouds and precipitation. Reviews of Geophysics 2012;50(2).

Tao WK, Li X, Khain A, Matsui T, Lang S, Simpson J. Role of atmospheric aerosol concentration on deep convective precipitation: Cloud-resolving model simulations. JGR: Atmospheres 2007;112(D24).

Tompkins A. The impact of dimensionality on long-term cloud-resolving model simulations. Monthly Weather Review 2000;128(5).

Tonttila J, Maalick Z, Raatikainen T, Kokkola H, Kühn T, Romakkaniemi S. Uclales-salsa v1. 0: a large-eddy model with interactive sectional microphysics for aerosol, clouds and precipitation. Geoscientific Model Development 2017;10(1):169.

Twomey S. Pollution and the planetary albedo. Atmospheric Environment 1974;8:1251–6.

Twomey SA. The influence of pollution on the shortwave albedo of clouds. Journal of the Atmospheric Sciences 1977;34(7):1149–52.

Verlinde J, Harrington JY, McFarquhar G, Yannuzzi V, Avramov A, Greenberg S, Johnson N, Zhang G, Poellot M, Mather JH, et al. The mixed-phase arctic cloud experiment. Bulletin of the American Meteorological Society 2007;88(2):205–22.